



# Effects of different doses of dezocine on central nervous system in mice

Wen-yi GONG<sup>1,2</sup>, Bing XU<sup>2</sup>, Li LIU<sup>2</sup>, Shi-tong LI<sup>1\*</sup> 

## Abstract

Dezocine is an opioid receptor agonist – antagonist gaining popularity in clinical practice. It is both  $\mu$ -receptor agonist and antagonist activities. This study was designed to investigate the effects of dezocine on the CNS oxidative and inflammation in mice. Eight-week old female BALB/c mice were obtained from Shanghai General Hospital of Nanjing Medical University animal center. All animal procedures were approved by the Animal Care and Use Committee of Nanjing Medical University. We found that increasing dose of dezocine induced oxidative stress and inflammation in multiple brain regions, including the prefrontal cortex, cerebellum, temporal cortex, and striatum. Elevated expression levels of anti-oxidants (NRF2, SOD-1 and HO-1), KEAP-1, GSH and MDA were found in the prefrontal cortex and striatum. Elevated HO-1 and NRF2 levels were detected in the cerebellum and temporal cortex in the 3.0 mg/kg dezocine treated group. The SOD-1, HO-1, KEAP-1, NRF2, GSH and MDA levels were similar among groups in the olfactory bulb. The prefrontal cortex and striatum showed the most elevated oxidative stress (NRF2, SOD-1, and HO-1) marker levels. The number of PV-positive interneurons was decreased in the 1.5 mg/kg dezocine treated group, while the number of PNNs steadily increased over 3.0 mg/kg dezocine treated.

**Keywords:** dezocine; central nervous system.

**Practical Application:** Influence of patient control intravenous analgesia (PCIA) using dezocine on breast milk and neonates.

## 1 Introduction

The central nervous system (CNS) is one of the most vulnerable structures to different kind of injuries such as toxic agents capable of crossing the blood–brain barrier. Microglia, the resident immune cells in the brain, play a pivotal role in immune surveillance of the central nervous system (CNS) (Pedersen et al., 2020; Postels et al., 2020; Vila et al., 2020). Consequently, these cells are likely to play an important role in either development of protective immune responses or progression of damaging inflammation during CNS disease states. Pathological states within the nervous system, including injury, ischemic stroke, and infection, can lead to microglial activation and production of a host of factors, including tumor necrosis factor- $\alpha$  (TNF- $\alpha$ ), prostaglandin E2 (PGE2), interleukin-6 (IL-6), nitric oxide (NO), and reactive oxygen species (ROS) (Guizar-Sahagun et al., 2017; Silveira et al., 2017; Sprenkle et al., 2017; Thompson & Tsirka, 2017). Accumulation of these proinflammatory and cytotoxic factors is deleterious directly to neurons and subsequently induces further activation of microglia, resulting in a vicious cycle (Appelgren et al., 2019; Arieli, 2019; Qian et al., 2019).

Dezocine is an opioid receptor agonist – antagonist gaining popularity in clinical practice because of its mild side effects and high efficacy as an analgesic. It is both  $\mu$ -receptor agonist and antagonist activities (Mao et al., 2020; Song et al., 2020). Studies have shown that dezocine is a more potent analgesic than morphine, pentazocine and codeine (Hoskin & Hanks, 1991). The administration of dezocine generates minimal side effects such as vomiting, nausea and drowsiness. Multiple studies have

shown that normal dose of dezocine causes no obvious respiratory depression and is better received by both patients and doctors. It has been demonstrated that the administration of opioids influences immune functions through T cells, natural killer cells, monocytes and neutrophils (Jiao & Liu, 2014; Li et al., 2015; Su et al., 2014).

In the CNS, microglial activation induces oxidative stress, inflammation, and the unfolded protein response. Blood–brain barrier damage, and degeneration of cortical neurons and glia, were found after microglial activation. Direct microglial activation may activate the oxidative stress pathway, leading to elevated antioxidant enzymes (e.g., superoxide dismutase) (Minami et al., 2019) and lipid peroxidation in the cerebellum and hippocampus. These oxidative stressors could subsequently cause increased expression of perineuronal nets (PNNs) to protect neurons against neurotoxic injury (Burket et al., 2017; Shi et al., 2019). However, the influences of dezocine on oxidative stress in the CNS are rarely reported. Therefore, this study was designed to investigate the effects of dezocine on the CNS oxidative and inflammation in mice. Our findings may provide new evidence for reasonable selection of opioids to in pain management.

## 2 Patients and methods

### 2.1 Animals

Eight-week old female BALB/c mice were obtained from Shanghai General Hospital of Nanjing Medical University animal

Received 20 July, 2021

Accepted 13 Oct., 2021

<sup>1</sup> Department of Anesthesiology, Shanghai General Hospital of Nanjing Medical University, Shanghai, China

<sup>2</sup> Department of Anesthesiology, Wusong Hospital, Shanghai, China

\*Corresponding author: ercolani@163.com

center. All animal procedures were approved by the Animal Care and Use Committee of Nanjing Medical University. Mice were intraperitoneally administrated with increasing doses (0.75, 1.5 and 3.0 mg/kg) of dezocine (Yangtze River Pharmaceutical Group, purity >99.9%), and their peripheral blood samples were collected at predetermined time points (0, 12, 24 and 48 h). At the end of the experimental period (4 weeks), fresh olfactory bulb, prefrontal cortex, temporal cortex, striatum, and cerebellum tissue (n = 5 for each exposure group) and whole brain tissue for immunostaining (n = 3 for each exposure group) were harvested. Under anesthesia, whole brain was obtained after cardiac perfusion with phosphate-buffered saline (PBS), followed by 4% paraformaldehyde (pH 7.4). The brains were immersion-fixed in the 4% paraformaldehyde solution. The fresh brain tissues were collected and were rapidly frozen on -20 °C dry ice. After micropunching each brain region of olfactory bulb, prefrontal cortex, temporal cortex, striatum, and cerebellum, mRNA and protein were extracted from the tissue punches for RT-PCR and western blotting, respectively.

## 2.2 Extract the total RNA

We use Recover All™ Total Nucleic Acid Isolation Kit to extract the Total RNA from tissue samples. The thickness of this sample is 10um and put these sample into a 1.5ml tube. Put the Xylene into the tube for the purpose is dissolve the wax and the protein is digested by the protease. Next step is extracting the Nucleic acid, the mixture liquid is filtered through filter column. For the purpose is use the RNA to go to the PCR. However, the collected liquid is contained DNA and RNA, and we use the DNase to degrade DNA so that make the sample pure. Finally, we put the Elution solution into Filter column to collect the RNA. We use the NANO DROP 2000 for quality assessment. The maximum absorption wavelength of nucleic acid is 260nm, which can be used to calculate the concentration of nucleic acid sample. The ratio of OD value at 260nm and 280nm can be determined to estimate the purity of nucleic acid. The result of our experiment is that the extracted RNA was higher in content, and 260/280 analysis indicated un-degraded RNA, with higher purity, without pollution of DNA.

## 2.3 Western blotting

Brain tissue was lysed in radioimmunoprecipitation assay (RIPA) buffer (Cell Signaling Technology, Danvers, MA, USA). Lysate buffer composed of 20 mM Tris-HCl (pH 7.5), 150 mM NaCl, 1 mM Na<sub>2</sub>EDTA, 1 mM EGTA, 1% NP-40, 1% sodium deoxycholate, 1 mM β-glycerophosphate, 1 mM Na<sub>3</sub>VO<sub>4</sub>, 1 μg/mL leupeptin, and protease inhibitor cocktail solution (Cell Signaling Technology). A Bio-Rad Protein Assay Kit was used to determine the protein concentration for each treatment. Approximately 25 μg of protein was separated by 12% sodium dodecyl sulfate-polyacrylamide gel electrophoresis (SDS-PAGE) and transferred to polyvinylidene difluoride (PVDF) membranes (Merck Millipore, Burlington, MA, USA). The membranes were soaked in blocking buffer (5% non-fat dry milk in Tris-buffered saline containing Tween-20 for 1 h at room temperature. They were then incubated with specific primary antibodies: KEAP-1 (rabbit monoclonal; Abcam, Cambridge, UK), NRF2 (rabbit polyclonal; Abcam), HO-1 polyclonal antibody (rabbit; Enzo Life Sciences, Farmingdale, NY, USA), and β-actin (D6A8, rabbit

mAb; Cell Signaling Technology). Immunoreactive proteins were detected with a horseradish peroxidase (HRP)-coupled secondary antibody (anti-rabbit IgG, HRP-linked antibody; Cell Signaling Technology) and were visualized using an enhanced chemiluminescence (ECL) kit (Bio-Rad). The protein bands were quantitated by densitometry using ImageJ gel analysis software (National Institutes of Health, Bethesda, MD, USA).

## 2.4 Histology of PNNs

The specimens were dehydrated and embedded in optimal cutting temperature solution. For histological examination, 40-μm sections of embedded tissue were cut on a rotary cryotome and mounted on glass slides. Immunohistochemistry was performed by washing free-floating sections three times for 5 min each in PBS. The tissue was then placed in 50% ethanol for 30 min. After a set of three 5-min washes in PBS, the sections were placed in 10% goat or donkey blocking serum (Vector Labs, Burlingame, CA, USA) for 1 h. Free-floating slices were then incubated overnight at 4 °C on a shaking table with a primary antibody (rabbit anti mouse). The following day, and after three 10-min washes in PBS, sections were incubated for 2 h in Donkey anti-Rabbit IgG (H + L) Highly Cross-Adsorbed, Alexa Fluor® 594 secondary antibody (Invitrogen, Carlsbad, CA, USA). After another PBS wash, the tissue was incubated overnight at 4 °C on a shaking table, but with fluorescein-labeled Wisteria floribunda agglutinin (WFA; 1:500; Vector Laboratories) in PBS containing 2% goat serum. The tissue was washed three additional times in PBS for 10 min per wash, and mounted onto slides. After drying, the slides were coverslipped. The densities of PV+, WFA+, and co-localized (PV+WFA) cells were calculated in the temporal cortex of three mice from each group. The temporal cortex (A1) was localized based on a mouse brain atlas (Science). Six A1 areas from each group were analyzed in a 777 × 777 μm area. Images were photographed using a TCS SP5II confocal microscope (Leica, Wetzlar, Germany). The numbers of single-labeled WFA-positive cells, single-labeled PV-positive cells, and cells with co-localized WFA with PV within the frame at 20× were counted in ImageJ (NIH). All cell counts and measurements were performed blind to study groups.

## 2.5 Statistical analysis

Continuous variables were expressed as mean ± SD (standard deviation) and compared using a two-tailed unpaired Student's t test; categorical variables were compared using χ<sup>2</sup> or Fisher analysis. A value of P < 0.05 was considered significant in all the analyses. Statistical analysis of continuous and categorical variables and ROC curve analysis were computed using MedCalc V.11.0.3.0 (MedCalc software, Mariakerke, Belgium).

## 3 Results

### 3.1 Dezocine promotes expression of markers related with oxidative stress and inflammation in mRNA levels

The mRNA expression levels of KEAP-1, NRF2, HO-1, SOD-1, GSH and MDA were detected among different doses of Dezocine (Figure 1). The NRF2 and HO-1 mRNA levels were elevated in the prefrontal cortex, cerebellum, temporal

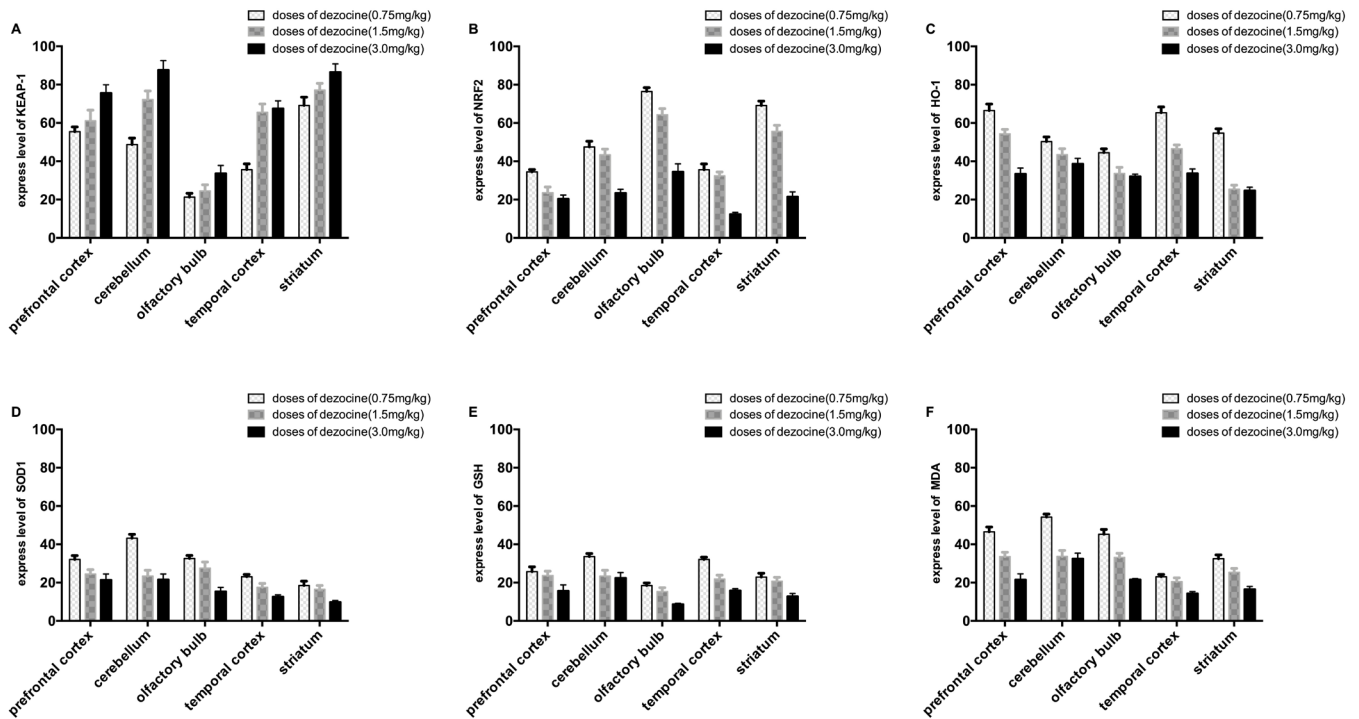


**Figure 1.** Dezocine promotes expression of markers related with oxidative stress and inflammation in mRNA levels.

cortex, and striatum in the 3.0 mg/kg dezocine treated group compared with the 0.75 and 1.5 mg/kg dezocine treated groups. KEAP-1 and SOD-1 mRNA expression was increased in the prefrontal cortex and striatum of the 3.0 mg/kg dezocine treated group compared with the 0.75 and 1.5 mg/kg dezocine treated groups. Higher SOD-1, GSH and MDA expression was detected in the prefrontal cortex and striatum of the 1.5 mg/kg dezocine treated group compared with the 0.75 mg/kg dezocine treated group (Figure 1). The expression of SOD-1, GSH and MDA were elevated in the cerebellum, temporal cortex, and striatum of the 3.0 mg/kg dezocine treated group.

### 3.2 Dezocine promotes expression of markers related with oxidative stress and inflammation in protein levels

The protein expression levels of KEAP-1, NRF2, HO-1, SOD-1, GSH and MDA were detected in cerebellum between 3.0 and 0.75 mg/kg dezocine treated groups (Figure 2). The NRF2 and HO-1 protein levels were elevated in the 3.0 mg/kg dezocine treated group compared with the 0.75 mg/kg dezocine treated group. KEAP-1 and SOD-1 protein expression was increased in the 3.0 mg/kg dezocine treated group compared with the 0.75 mg/kg dezocine treated group. Higher SOD-1, GSH and MDA expression were detected in the cerebellum of the 3.0 mg/kg dezocine treated group compared with the 0.75 mg/kg dezocine treated group (Figure 2).

### 3.3 Changes in PNNs and PV-positive interneurons

Changes in PNNs and related interneurons were examined in the temporal cortex, because elevated HO-1 and NRF2 expression

were observed in the temporal cortex of the 3.0 mg/kg dezocine treated group. The number of WFA-positive cells in the temporal cortex gradually increased after treated with dezocine (Figure 3). WFA-positive cells were significantly denser in the 3.0 mg/kg dezocine treated group compared with the 0.75 and 1.5 mg/kg dezocine treated groups. Fewer PV-positive cells were detected in the temporal cortex in the 1.5 mg/kg dezocine treated group compared with the 0.75 mg/kg dezocine treated group. The density of PV-positive cells was increased in the 3.0 mg/kg dezocine treated group; however, the density was less than that found in the 0.75 mg/kg dezocine treated group. The number of WFA + PV-positive cells was decreased in the 1.5 mg/kg dezocine treated group, but recovered in the 3.0 mg/kg dezocine treated group.

## 4 Discussion

The potential hazards of dezocine exposure, particularly with respect to the central nervous system (CNS), have recently attracted great interest. Dezocine exposure could contribute to the pathogenesis of neurodevelopmental disorders and neurodegenerative diseases, including autism spectrum disorder, Alzheimer's disease and Parkinson's disease. Dezocine have been detected in neurons, glia, the choroid plexus, the endothelium, the nasal and olfactory epithelium, and cerebrospinal fluid (Morgan et al., 1999; Walker et al., 1999); these metabolites from dezocine are associated with mitochondrial dysfunction, accumulation and aggregation of unfolded proteins, and abnormal endosomal systems. Following fine dezocine exposure, mice reportedly displayed depressive-like responses and impairments in spatial learning and memory (Huang et al., 2018; Li et al., 2017).

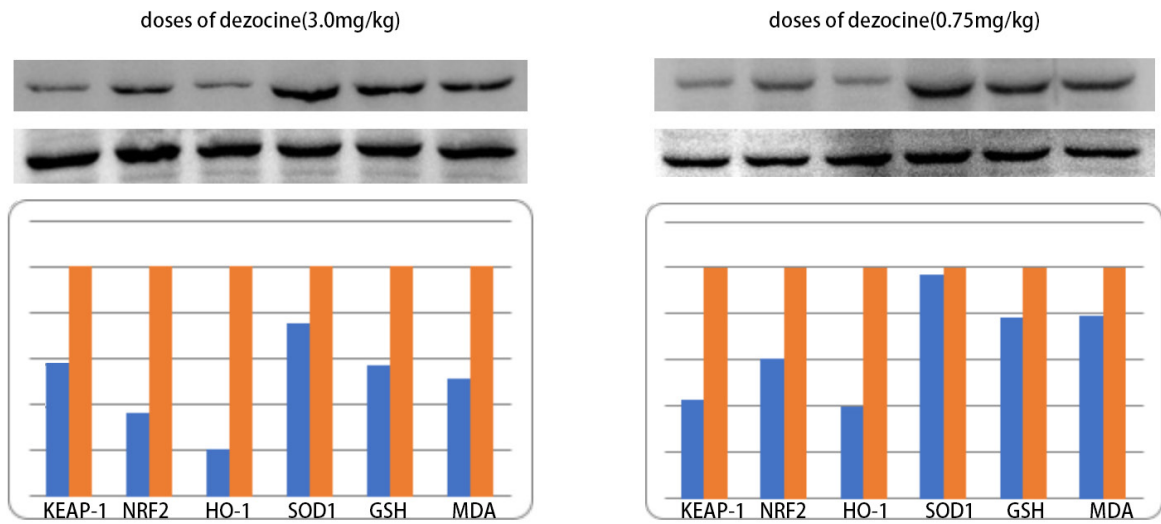


Figure 2. Dezocine promotes expression of markers related with oxidative stress and inflammation in protein levels.

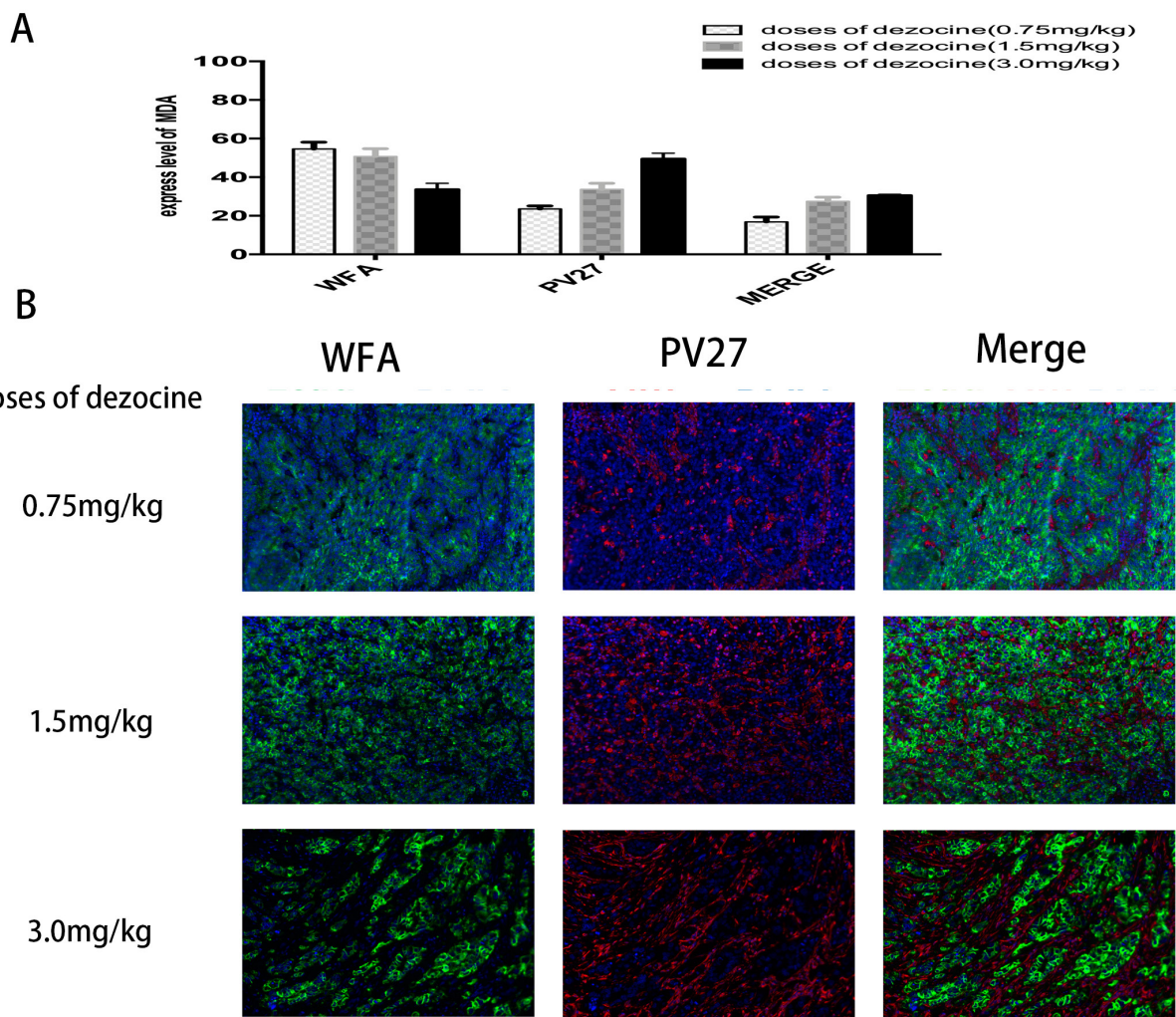


Figure 3. Changes in PNNs and related interneurons were examined in the temporal cortex, because elevated HO-1 and NRF2 expression were observed in the temporal cortex of the 3.0 mg/kg dezocine treated group.

As a mixed agonist-antagonist, dezocine mainly activate the kappa receptor, which generate sedative and analgesic effects. However, the kappa receptor agonist does not inhibit gastric emptying and small intestinal motility after intraperitoneal injection, while it inhibits the contraction of the colon by acting on the central. It was observed that dezocine did not elevate the muscle tone of the ileocecal sphincter in cats. Consistently, our study demonstrated that dezocine caused a slight increase in intestinal smooth muscle contraction and frequency in vitro.

In present study, we found that increasing dose of dezocine induced oxidative stress and inflammation in multiple brain regions, including the prefrontal cortex, cerebellum, temporal cortex, and striatum. Elevated expression levels of anti-oxidants (NRF2, SOD-1 and HO-1), KEAP-1, GSH and MDA were found in the prefrontal cortex and striatum. Elevated HO-1 and NRF2 levels were detected in the cerebellum and temporal cortex in the 3.0 mg/kg dezocine treated group. The SOD-1, HO-1, KEAP-1, NRF2, GSH and MDA levels were similar among groups in the olfactory bulb. Few previous studies investigated CNS effects of chronic exposure to dezocine; the present study revealed dezocine-induced regional differences and temporal changes in oxidative stress, inflammation, and neural proliferation. Furthermore, changes in PNNs and PV-positive neurons were detected for various periods of dezocine.

However, there are limitations of this study: (1)the sample size is too small in this study, and further larger sample studies are needed to confirm the present results; (2)the deeply mechanism of dezocine on the CNS through oxidative stress also needs future confirmation.

In conclusion, 3.0 mg/kg dezocine treated mice resulted in increased oxidative stress and inflammation in multiple brain regions. The prefrontal cortex and striatum showed the most elevated oxidative stress (NRF2, SOD-1, and HO-1) marker levels. The number of PV-positive interneurons was decreased in the 1.5 mg/kg dezocine treated group, while the number of PNNs steadily increased over 3.0 mg/kg dezocine treated.

## Conflict of interest

None.

## References

Appelgren, D., Enocsson, H., Skogman, B. H., Nordberg, M., Perander, L., Nyman, D., Nyberg, C., Knopf, J., Muñoz, L. E., Sjöwall, C., & Sjöwall, J. (2019). Neutrophil Extracellular Traps (NETs) in the cerebrospinal fluid samples from children and adults with central nervous system infections. *Cells*, 9(1), 43. <http://dx.doi.org/10.3390/cells9010043>. PMID:31877982.

Arieli, R. (2019). Calculated risk of pulmonary and central nervous system oxygen toxicity: a toxicity index derived from the power equation. *Diving and Hyperbaric Medicine*, 49(3), 154-160. <http://dx.doi.org/10.28920/dhm49.3.154-160>. PMID:31523789.

Burket, J. A., Urbano, M. R., & Deutsch, S. I. (2017). Sugarcoated perineuronal nets regulate "GABAergic" transmission: bittersweet hypothesis in autism spectrum disorder. *Clinical Neuropharmacology*, 40(3), 120-130. <http://dx.doi.org/10.1097/WNF.0000000000000209>. PMID:28277443.

Guizar-Sahagun, G., Martinez-Cruz, A., Franco-Bourland, R. E., Cruz-Garcia, E., Corona-Juarez, A., Diaz-Ruiz, A., Grijalva, I., Reyes-Alva, H. J., & Madrazo, I. (2017). Creation of an intramedullary cavity by hemorrhagic necrosis removal 24 h after spinal cord contusion in rats for eventual intralaminar implantation of restorative materials. *PLoS One*, 12(4), e0176105. <http://dx.doi.org/10.1371/journal.pone.0176105>. PMID:28414769.

Hoskin, P. J., & Hanks, G. W. (1991). Opioid agonist-antagonist drugs in acute and chronic pain states. *Drugs*, 41(3), 326-344. <http://dx.doi.org/10.2165/00003495-199141030-00002>. PMID:1711441.

Huang, Y. Q., Guo, S. H., Liu, R., Zhu, S. M., Sun, J. L., & Yao, Y. X. (2018). Additive analgesic effect of dexmedetomidine and dezocine administered intrathecally in a mouse pain model. *Oncotarget*, 9(36), 24391-24397. <http://dx.doi.org/10.18632/oncotarget.25304>. PMID:29849948.

Jiao, L., & Liu, R. C. (2014). Effects of dezocine on postoperative sore throat after maxillofacial procedures: a comparison with flurbiprofen axetil. *Beijing Da Xue Xue Bao. Yi Xue Ban*, 46(1), 104-106. PMID:24535359.

Li, N. N., Huang, Y. Q., Huang, L. E., Guo, S. H., Shen, M. R., Guo, C. L., Zhu, S. M., & Yao, Y. X. (2017). Dezocine antagonizes morphine analgesia upon simultaneous administration in rodent models of acute nociception. *Pain Physician*, 20(3), E401-E409. PMID:28339439.

Li, X., Xia, Q., & Li, W. (2015). Comparison of the effects of dezocine, fentanyl, and placebo on emergence agitation after sevoflurane anesthesia in children. *International Journal of Clinical Pharmacology and Therapeutics*, 53(3), 241-246. <http://dx.doi.org/10.5414/CP202184>. PMID:25669611.

Mao, X. F., Ahsan, M. Z., Apriyani, E., Tang, X. Q., Zhao, M. J., Li, X. Y., & Wang, Y. X. (2020). Dual mu-opioid receptor and norepinephrine reuptake mechanisms contribute to dezocine- and tapentadol-induced mechanical allodynia in cancer pain. *European Journal of Pharmacology*, 876, 173062. <http://dx.doi.org/10.1016/j.ejphar.2020.173062>. PMID:32173379.

Minami, S., Miura, K., Ishioka, M., Morimoto, N., Isoda, N., Yamamoto, H., & Iijima, K. (2019). Homocysteine supplementation ameliorates steatohepatitis induced by a choline-deficient diet in mice. *Hepatology Research*, 49(2), 189-200. <http://dx.doi.org/10.1111/hepr.13234>. PMID:30048033.

Morgan, D., Cook, C. D., Smith, M. A., & Picker, M. J. (1999). An examination of the interactions between the antinociceptive effects of morphine and various mu-opioids: the role of intrinsic efficacy and stimulus intensity. *Anesthesia and Analgesia*, 88(2), 407-413. <http://dx.doi.org/10.1097/0000539-199902000-00035>. PMID:9972766.

Pedersen, E. M. J., Kohler-Forsberg, O., Nordentoft, M., Christensen, R. H. B., Mortensen, P. B., Petersen, L., & Benros, M. E. (2020). Infections of the central nervous system as a risk factor for mental disorders and cognitive impairment: a nationwide register-based study. *Brain, Behavior, and Immunity*, 88, 668-674. <http://dx.doi.org/10.1016/j.bbi.2020.04.072>. PMID:32353515.

Postels, D. G., Osei-Tutu, L., Seydel, K. B., Xu, Q., Li, C., Taylor, T. E., John, C. C., Mallewa, M., Solomon, T., Agbenyega, T., Ansong, D., Opoka, R. O., Khan, L. M., Ramachandran, P. S., Leon, K. E., DeRisi, J. L., Langelier, C., & Wilson, M. R. (2020). Central nervous system virus infection in african children with cerebral malaria. *The American Journal of Tropical Medicine and Hygiene*, 103(1), 200-205. <http://dx.doi.org/10.4269/ajtmh.19-0962>. PMID:32342847.

Qian, X., Li, X., Shi, Z., Bai, X., Xia, Y., Zheng, Y., Xu, D., Chen, F., You, Y., Fang, J., Hu, Z., Zhou, Q., & Lu, Z. (2019). KDM3A senses oxygen availability to regulate PGC-1alpha-mediated mitochondrial

- biogenesis. *Molecular Cell*, 76(6), 885-895. <http://dx.doi.org/10.1016/j.molcel.2019.09.019>. PMID:31629659.
- Shi, W., Wei, X., Wang, X., Du, S., Liu, W., Song, J., & Wang, Y. (2019). Perineuronal nets protect long-term memory by limiting activity-dependent inhibition from parvalbumin interneurons. *Proceedings of the National Academy of Sciences of the United States of America*, 116(52), 27063-27073. <http://dx.doi.org/10.1073/pnas.1902680116>. PMID:31843906.
- Silveira, E. L. V., Rogers, K. A., Gumber, S., Amancha, P., Xiao, P., Woollard, S. M., Byrareddy, S. N., Teixeira, M. M., & Villinger, F. (2017). Immune cell dynamics in rhesus macaques infected with a Brazilian strain of Zika Virus. *Journal of Immunology*, 199(3), 1003-1011. <http://dx.doi.org/10.4049/jimmunol.1700256>. PMID:28667164.
- Song, Q., Liu, G., Liu, D., & Feng, C. (2020). Dezocine promotes T lymphocyte activation and inhibits tumor metastasis after surgery in a mouse model. *Investigational New Drugs*, 38(5), 1342-1349. <http://dx.doi.org/10.1007/s10637-020-00921-6>. PMID:32170576.
- Sprenkle, N. T., Sims, S. G., Sanchez, C. L., & Meares, G. P. (2017). Endoplasmic reticulum stress and inflammation in the central nervous system. *Molecular Neurodegeneration*, 12(1), 42. <http://dx.doi.org/10.1186/s13024-017-0183-y>. PMID:28545479.
- Su, Z., Zhang, Y., Liu, Y., An, L. J., & Liu, H. L. (2014). The effect of dezocine in prevention of adverse reaction of tracheal extubation in nasal endoscopic operation. *Zhongguo Ying Yong Sheng Li Xue Za Zhi*, 30(5), 394-395, 400. PMID:25571627.
- Thompson, K. K., & Tsirka, S. E. (2017). The diverse roles of microglia in the neurodegenerative aspects of Central Nervous System (CNS) autoimmunity. *International Journal of Molecular Sciences*, 18(3), 504. <http://dx.doi.org/10.3390/ijms18030504>. PMID:28245617.
- Vila, J., Bosch, J., & Munoz-Almagro, C. (2020). Molecular diagnosis of the central nervous system (CNS) infections. *Enfermedades Infecciosas y Microbiología Clínica*. <http://dx.doi.org/10.1016/j.eimc.2020.03.001>. PMID:32345489.
- Walker, E. A., Tiano, M. J., Benyas, S. I., Dykstra, L. A., & Picker, M. J. (1999). Naltrexone and beta-funaltrexamine antagonism of the antinociceptive and response rate-decreasing effects of morphine, dezocine, and d-propoxyphene. *Psychopharmacology*, 144(1), 45-53. <http://dx.doi.org/10.1007/s002130050975>. PMID:10379623.